Immunity
Resource

In Vivo RNA Interference Screens Identify Regulators of Antiviral CD4$^+$ and CD8$^+$ T Cell Differentiation

Runqiang Chen,[1,2,3,5] Simon Bélanger,[2,5] Megan A. Frederick,[3] Bin Li,[2] Robert J. Johnston,[2] Nengming Xiao,[4] Yun-Cai Liu,[4] Sonia Sharma,[4] Bjoern Peters,[2] Anjana Rao,[1] Shane Crotty,[2,*] and Matthew E. Pipkin[3,*]
[1]Division of Signaling and Gene Expression, La Jolla Institute for Allergy and Immunology, La Jolla, CA 92037, USA
[2]Division of Vaccine Discovery, La Jolla Institute for Allergy and Immunology, La Jolla, CA 92037, USA
[3]Department of Cancer Biology, The Scripps Research Institute, Jupiter, FL 33458, USA
[4]Division of Cell Biology, La Jolla Institute for Allergy and Immunology, La Jolla, CA 92037, USA
[5]Co-first author
*Correspondence: shane@lji.org (S.C.), mpipkin@scripps.edu (M.E.P.)
http://dx.doi.org/10.1016/j.immuni.2014.08.002

SUMMARY

Classical genetic approaches to examine the requirements of genes for T cell differentiation during infection are time consuming. Here we developed a pooled approach to screen 30–100+ genes individually in separate antigen-specific T cells during infection using short hairpin RNAs in a microRNA context (shRNAmir). Independent screens using T cell receptor (TCR)-transgenic CD4$^+$ and CD8$^+$ T cells responding to lymphocytic choriomeningitis virus (LCMV) identified multiple genes that regulated development of follicular helper (Tfh) and T helper 1 (Th1) cells, and short-lived effector and memory precursor cytotoxic T lymphocytes (CTLs). Both screens revealed roles for the positive transcription elongation factor (P-TEFb) component Cyclin T1 (*Ccnt1*). Inhibiting expression of Cyclin T1, or its catalytic partner Cdk9, impaired development of Th1 cells and protective short-lived effector CTL and enhanced Tfh cell and memory precursor CTL formation in vivo. This pooled shRNA screening approach should have utility in numerous immunological studies.

INTRODUCTION

The differentiation of T cells into effector and memory cells is central to adaptive immunity. Transcription factors (TFs) are central regulators of these differentiation processes. Although most current models of T cell differentiation incorporate relatively few regulatory players and rely heavily on the "master regulator" concept, it is abundantly clear that TFs do not act in isolation and that transcription programs that underlie cell differentiation require the concerted actions of multiple factors, including important inducers or repressors of T cell differentiation pathways (Crotty, 2012; Kaech and Cui, 2012; O'Shea and Paul, 2010; Oestreich and Weinmann, 2012; Pipkin and Rao, 2009; Walsh et al., 2002). One large-scale study of the regulation of gene expression in different cell types and tissues found that a given murine cell type could be distinguished from other cell types by a network of approximately six TF:TF interactions and that these TF networks were conserved in human cell types (Ravasi et al., 2010). Thus, the intersecting expression and actions of multiple TFs appear to determine cell fate and function. Recent work on T helper 17 (Th17) cell differentiation suggests that this model also applies to T cells (Ciofani et al., 2012).

The differentiation of naive CD8$^+$ T cells into CTLs is a key process in immunity to viral infections. The differential development of short-lived effector CTLs and precursors to long-lived memory CTLs are considered alternative cellular "fates" (Chang et al., 2007; Joshi et al., 2007), and understanding this process is critical for prevention and treatment of acute and chronic infections (Doering et al., 2012; Haining and Wherry, 2010; Kaech and Cui, 2012). Activated CD4$^+$ T cells can differentiate into a range of different functional subsets, including Th1, Th2, Th17, peripheral Treg (pTreg), and follicular helper (Tfh) cells, which each have potent capacities to regulate immune responses and eliminate pathogens. Among CD4$^+$ T cells, follicular T helper cells (Tfh) are the specialized providers of help to B cells (Crotty, 2011). T-cell-dependent antibody responses are important for protection against a wide range of pathogens. Our understanding of Tfh cells is still in the early stages, and there is much to be learned about the pathways that control Tfh cell differentiation.

A number of excellent studies have characterized the mRNA expression profiles of CD8$^+$ and CD4$^+$ T cells isolated ex vivo during the course of antigen-specific responses (Best et al., 2013; Doering et al., 2012; Kaech and Cui, 2012; Kalia et al., 2010; Choi et al., 2013). However, differential mRNA expression studies are likely to overlook a large number of relevant factors responsible for T cell differentiation. For example, of nearly 2,000 predicted conventional DNA-binding transcription factors in the murine genome (Gray et al., 2004), fewer than 15 have validated roles in effector CD8$^+$ T cell differentiation (Kaech and Cui, 2012; Pipkin and Rao, 2009). The same limitations probably hold for Tfh cell differentiation and other CD4$^+$ T cell differentiation pathways (Crotty, 2012; Oestreich and Weinmann, 2012; Vahedi et al., 2013). Thus, a functional genetic approach in which inhibition of a large number of genes individually, in separate cells in parallel, during T cell differentiation has the potential to rapidly

identify factors comprising the genetic networks underlying T cell function.

To pursue this objective, we have devised an experimental approach that uses retroviral shRNAmir libraries to diminish the expression of selected gene products one at a time in antigen-specific T cells. Gene function in antiviral responses is then interrogated in pooled screens in mice. We have demonstrated the utility of this approach in two T cell differentiation processes in vivo: $CD8^+$ T cell differentiation into cytotoxic T lymphocytes (CTLs) and $CD4^+$ T cell differentiation into Tfh and Th1 cells. Here we showed proof of principle that the roles of multiple genes can be interrogated in parallel in T cells during infection and identified previously unappreciated factors that were involved in these differentiation processes. This approach holds promise to substantially accelerate the understanding of T cell differentiation in vivo.

RESULTS

An Optimized Retroviral Vector to Express shRNAmirs In Vivo

Transduction of activated T cells with murine stem cell virus (MSCV)-based retroviral expression vectors (RVs) has previously been used to drive transgene expression or to deplete expression of endogenous genes by triggering RNA interference (RNAi) using shRNAs upon adoptive transfer in vivo (Araki et al., 2009; Johnston et al., 2009; Joshi et al., 2007; Kao et al., 2011). However, we found that transduction of SMARTA TCR transgenic CD4 T cells (LCMV-specific, gp66-77 IA^b restricted) with an MSCV-based (pLMP-derived) RV designed to express shRNAs in the context of miRNA-30 sequences (shRNAmir) resulted in depletion of the transduced cells after an acute LCMV infection (Figure S1A, left, available online). This most likely was due to immune rejection of antigens expressed from pLMP (Figure S1B), because deletion of the puromycin resistance gene from pLMP (LMPd) eliminated this effect (Figure S1A, right). We replaced GFP in LMPd with the violet-excitable, yellow-fluorescing GFP variant Ametrine1.1 (LMP-Amt) to expand its utility in FACS (Figures S1B and S1C) and confirmed its functionality for RNAi in vivo by targeting *Bcl6* transcripts. Transferred SMARTA $CD4^+$ T cells transduced with *Bcl6*-specific shRNAs (LMP-Amt sh*Bcl6*-RV, referred to hereafter as sh*Bcl6*-RV) displayed a reduced fraction of $CXCR5^+Bcl6^+$ cells upon LCMV infection, consistent with a requirement for *Bcl6* for differentiation of follicular T helper cells (Tfh) (Figure S1D).

A Pooled Screening System using shRNAs in $CD8^+$ T Cells during LCMV Infection

We parallelized the shRNAmir-RV approach in order to interrogate the functions of numerous genes simultaneously. The experimental strategy was to introduce a pool of TCR transgenic T cells carrying individual shRNAs into host mice and assay alterations in the composition of shRNAs carried by the responding T cells during a viral infection (Figure 1A). In effect, each T cell is barcoded by the integrated shRNA-RV, and the fate of individual cells carrying each shRNA can be monitored in T cell populations of interest by deep sequencing DNA libraries derived from the integrated provirus (Figures 1B and 1C; Beronja et al., 2013; Zuber et al., 2011). We optimized conditions in 96-well format to produce arrays of high-titer RV supernatants without concentration, sufficient to transduce $\geq$70% of LCMV-specific P14 TCR transgenic $CD8^+$ T cells 18 hr after TCR stimulation (Figures 1B, S2A, and S2B). The day after transduction, cells from each well were pooled (Figure 1B, day 0) and immediately transferred to recipient mice without cell sorting (sorting reduced P14 accumulation in vivo; Figure S2C), and the recipients were infected with LCMV 1 hr later. In addition, an aliquot of Ametrine-high cells was FACS purified and saved as the "input."

Genomic DNA was prepared from the input and samples of P14 cells isolated by flow cytometry on day 7 after LCMV infection. Deep sequencing was used to quantify shRNA representation (Figures 1A and S2D–S2H) in libraries generated from a single-step PCR of the shRNAmir sequences in genomic DNA template (Figures 1B and 1C). Multiple PCR conditions were interrogated (Figures S2D–S2G). Independent libraries generated from different DNA template amounts at low PCR cycles (22 or 26 cycles; Figures S2F and S2G) exhibited high correlations in shRNA representation, with both 314 (medium-density) and 318 (high-density) PGM sequencing chips (Figure S2H). Thus, the sequencing approach was robust.

To establish conditions for screening pools of shRNAmir-RV^+ P14 $CD8^+$ T cells in the context of infection, numerous factors were optimized and standardized (Figure S3). Naive $Thy1.1^+$ Blimp1-YFP transgenic P14 cells were activated in vitro and transferred to B6 hosts subjected to LCMV infection and the P14 cells were examined as a function of (1) cell transfer number (Figure S3A), (2) the timing of the infection relative to cell transfer (data not shown), (3) LCMV dose (Figure S3B), and (4) LCMV strain (Figure S3C). Transfer of 500,000 activated P14 cells followed by intraperitoneal (i.p.) infection with 1.5×10^5 PFU of LCMV-clone 13 (LCMV-cl13) resulted in a robust infection that induced accumulation of $\sim 10^6$ P14 cells in the spleen by day 7, ~50-fold more than in uninfected recipients (Figures 1D and S3D). Under these conditions virus replication was strongly inhibited (see below), and the responding P14 cells exhibited $CD8^+$ T cell phenotypes typical of acute infection, based on interleukin-2 receptor α (IL-2Rα) (CD25), KLRG-1, IL-7Rα (CD127), and Blimp1-YFP reporter expression (Figures 1E, 1F, and S4A). LCMV-cl13 is more virulent than LCMV Armstrong (Wherry et al., 2003) but was controlled due to the P14 cell transfers. In addition, we confirmed that short-lived effector (KLRG-1^{hi}IL-$7R\alpha^{lo}$) and memory precursor (KLRG-1^{lo}IL-$7R\alpha^{hi}$) P14 populations exhibited different potentials for memory cell formation and "recall" capacity (Figures S4B–S5E). Altogether, these results demonstrate robust conditions with which to screen effector and memory CTL development.

The number of distinct shRNAmirs that could be tested in parallel was constrained by the number of adoptively transferred T cells. In order to ensure library complexity, we aimed to represent each shRNA with ~500 cells per mouse upon engraftment. This depth of representation is similar to or exceeds recent in vivo shRNA-based screens (Beronja et al., 2013; Zhou et al., 2014; Zuber et al., 2011). Based on data from adoptively transferred naive $CD8^+$ T cells (Badovinac et al., 2007) and activated $CD8^+$ T cells (Pipkin et al., 2010), we assumed that ~10% of transferred cells would engraft. Thus, we initially analyzed a pool of 500,000 cells representing ~100 unique shRNAs in a single experiment. We also considered the recovery of effector and

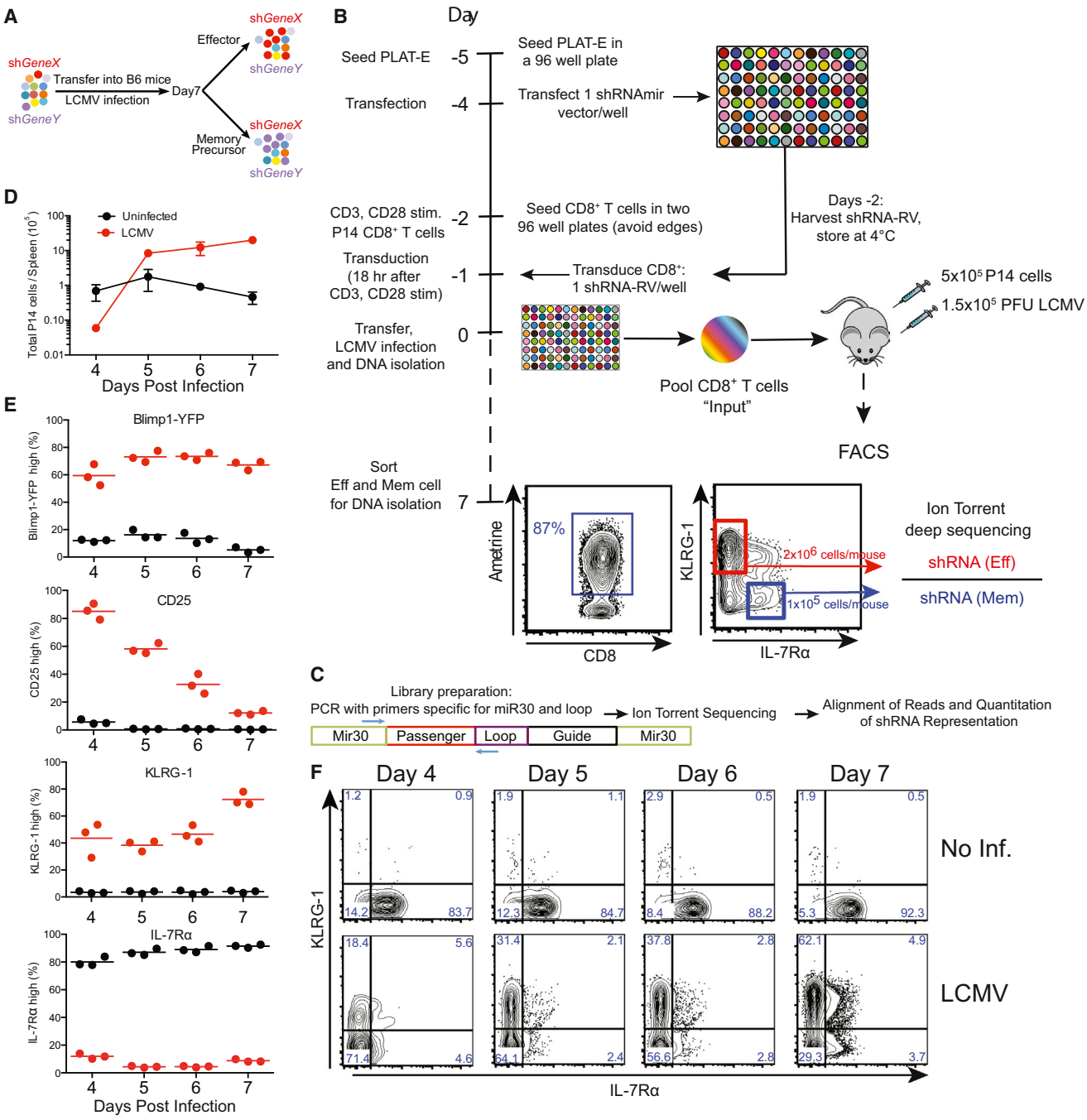

Figure 1. Optimization of Conditions for a Pooled Screening Approach using shRNAmirs in CD8+ T Cells In Vivo to Identify Genes that Regulate CTL Differentiation during Infection

(A) A conceptual representation depicting the principle of the pooled screening strategy.

(B) Scheme for the shRNAmir screen using P14 cells and LCMV infection.

(C) Scheme for quantifying shRNAmirs. DNA libraries generated by PCR of the integrated shRNAmir provirus are analyzed by deep sequencing to quantify shRNA representation in the cell subsets.

(D) Total P14 cell numbers recovered in the spleen in the presence or absence of LCMV infection. Error bars indicate standard deviations.

(E) Blimp1-YFP^{hi}, CD25^{hi}, KLRG-1^{hi}, and IL-7Rα^{hi} cell frequencies at the indicated time points after infection. Symbols represent values from individual mice. Red indicates LCMV-infected mice; black indicates uninfected mice.

(F) Representative flow cytometry plots of KLRG-1 and IL-7Rα staining on P14 cells under conditions used for screening.

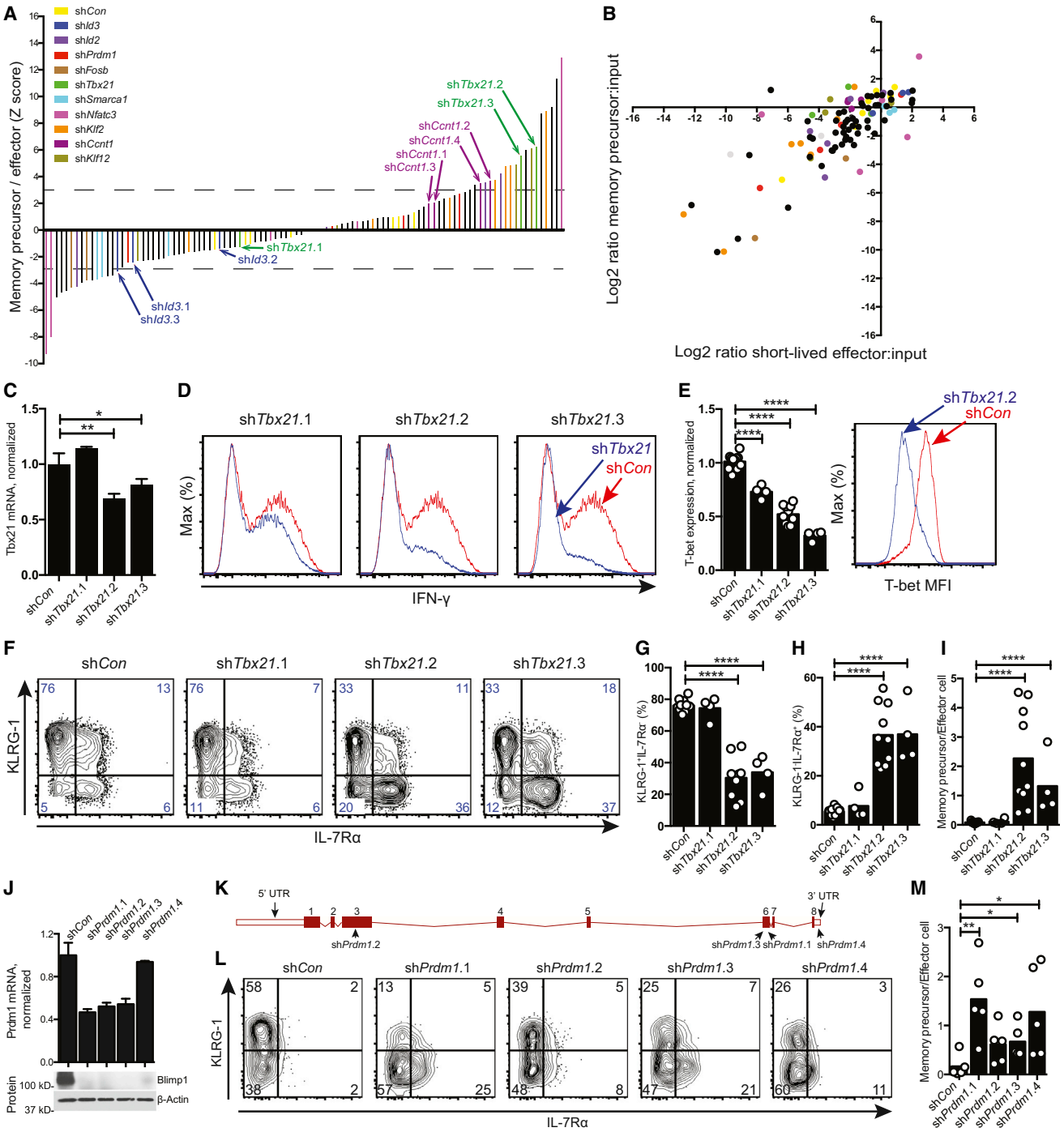

Figure 2. A Pooled RNAi Screen in CD8+ T Cells In Vivo Identifies Potential Regulators of Effector and Memory Precursor CTL Formation

(A) Relative enrichment of shRNAs in memory precursor and short-lived effector P14 cell populations is reported as Z-scores for each shRNA in the library. Each bar represents a single shRNA. Negative control shRNAs are colored yellow.

(B) Scatter plot shows the $\log_2$ ratio of normalized reads of all shRNAs in each sorted CD8+ T cell subset versus the input sample. Each dot represents a unique shRNA and is color coded as in (A).

(C) *Tbx21* mRNA expression in sh*Tbx21*+ P14 CD8+ T cells, after 6 days of culture (10 U/ml IL-2). Abbreviation is as follows: sh*Con*, control shRNAmir.

(D) Intracellular IFN-γ staining in P14 CD8+ T cells, gated on sh*Tbx21*+ cells. Cells were cultured for 6 days (10 U/ml IL-2) and restimulated with PMA and ionomycin for 4 hr before staining.

(E) T-bet expression in sh*Tbx21*+ P14 CD8+ T cells from spleens 8 days after LCMV infection (normalized geometric MFI). T-bet staining is shown for representative mice (right).

(F) Contour plots show KLRG-1 and IL-7Rα staining on sh*Tbx21*+ P14 CD8+ T cells from representative mice 8 days after LCMV infection.

(legend continued on next page)

memory precursor populations. Based on P14 accumulation data at day 7 postinfection (Figure 1D), we expected to recover ~300,000 KLRG-1^{hi}IL-7Rα^{lo} and ~30,000 KLRG-1^{lo}IL-7Rα^{hi} cells per mouse. To assure that cell numbers would not limit library complexity at the end of the experiment and to reduce potential founder effects from variation in individual mice (Zuber et al., 2011), sorted cells were pooled from five or more infected mice in each experiment.

Identification of Genes Underlying CTL Differentiation by an shRNA Screen In Vivo

We selected 34 genes to screen to test the approach. These included genes differentially expressed in Tfh cells and CTLs (Choi et al., 2013), broadly expressed chromatin and transcriptional regulators with unknown roles in effector T cells, and multiple positive and negative control genes. Each gene was targeted by 1–5 shRNAmirs, depending on availability in the original library (see Experimental Procedures and Table S1). The use of multiple shRNAs per gene is important, to control for off-target effects, and not all shRNAs are functional. A total of 110 unique shRNAs that target these genes were subcloned as a pool into pLMPd-Amt (Table S1 and Figures S5A and S5B). Individual colonies from this transformation were picked, sequence verified, and rearrayed into 96-well plates.

Retroviral supernatants prepared from cells transfected with the array of 110 shRNAmir DNAs were used to transduce P14 cells. Transduction of each construct was confirmed by Ametrine fluorescence, and P14 cells were pooled. An aliquot was removed for the input sample, and 500,000 cells were transferred into multiple recipient mice that were then infected with LCMV. On day 7 postinfection, short-lived effector (KLRG-1^{hi}IL-7Rα^{lo}) and memory precursor (KLRG-1^{lo}IL-7Rα^{hi}) P14 cells were sorted, genomic DNA was extracted from each population, and shRNAmir sequencing libraries were prepared. After sequencing and alignment to the reference shRNA sequences, 642,718 (input), 233,902 (effector), and 487,865 (memory) mapped reads were retained for each cell susbset. All intended shRNAs introduced during T cell transduction were recovered from input samples; only two were not detected in either the effector or memory precursor cell populations. The memory precursor:short-lived effector cell ratio for each shRNA was calculated. Values from negative control shRNAs targeting genes not expressed in CD8$^+$ T cells (*Cd4*, *Cd14*, *Cd19*, *Ms4a1* [CD20]) based on RNA-seq analysis (M.E.P., unpublished data) were used to calculate *Z*-scores for each shRNA (Figure 2A and Table S1) and the ratios of shRNAs in effector and memory precursor subsets relative to the input cells was plotted (Figure 2B). Several shRNAs were substantially reduced in both short-lived effector and memory precursor P14 cell subsets relative to input, suggesting that genes they affected were required for the accumulation of P14 T cells during infection (Figure 2B).

To focus on factors with differential effects on short-lived effector versus memory precursor CD8$^+$ T cell subsets, we identified genes for which two or more cognate shRNAs were enriched with Z-score values of $\geq|3.0|$ and classified these as hits. None of the negative control genes exhibited this pattern (Figure 2A and Table S1). Genes that met these criteria were identified in both effector and memory precursor subsets (Figure 2A and Table S1). As expected from studies with gene-deficient mice (Cannarile et al., 2006; Intlekofer et al., 2005; Joshi et al., 2007; Yang et al., 2011), *Tbx21* (T-bet)- and *Id2*-specific shRNAs were enriched in memory precursor cells, because these genes are necessary for effector CTL generation (Figure 2A and Table S1). Conversely, all three *Id3*-specific shRNAs were enriched in effector CTLs (Figure 2A and Table S1), but just below the criteria to be designated a hit, consistent with a mild early defect in memory precursor formation in *Id3*-deficient mice (Ji et al., 2011; Yang et al., 2011).

Tbx21 and *Prdm1* shRNAs Impair Effector CTL Development during LCMV Infection

We validated results of the screen by examining the impact of shRNAs individually. Both sh*Tbx21*.2 and sh*Tbx21*.3, but not sh*Tbx21*.1, strongly depleted *Tbx21* mRNA and T-bet protein (Figures 2C and 2E), inhibited interferon-γ (IFN-γ) expression (Figure 2D), and limited development of short-lived effector cells in vivo ($p < 0.01$, Figures 2F–2I). These results correlated directly with the enrichment of these shRNAs in the screen (Figure 2A and Table S1) and confirmed the role of T-bet in the generation of effector CD8$^+$ T cells.

Prdm1 (encoding Blimp-1) has known roles in effector CD8$^+$ and CD4$^+$ T cell differentiation (Rutishauser et al., 2009; Shin et al., 2009; Johnston et al., 2009). Consistent with this, *Prdm1* shRNAs were preferentially enriched in memory precursor CD8$^+$ T cells, but the magnitude of their effects differed in replicates of the in vivo screen (Figure S5C and Table S1). Analysis of each *Prdm1* shRNA individually showed that three of four shRNAs impaired expression of both Blimp-1 mRNA and protein (Figure 2J). The fourth shRNA impaired Blimp-1 protein expression but did not reduce its mRNA (Figure 2J), perhaps because it targeted the *Prdm1* 3′ UTR (Figure 2K). Individually, all four *Prdm1* shRNAs impaired effector CD8$^+$ T cell frequencies and increased the ratio of memory precursor cells to short-lived effector cells in vivo ($p < 0.01$–0.05, Figures 2L and 2M). These data indicate that shRNAs can have variable effects but

(G–I) Quantitation of CD8$^+$ T cell subsets resulting from sh*Tbx21*$^+$ P14 cells in vivo.
(G) Short-lived effector cells (KLRG-1^{hi}IL-7Rα^{lo}).
(H) Memory precursor cells (KLRG-1^{lo}IL-7Rα^{hi}).
(I) Ratio of memory precursor to short-lived effector phenotype P14 cells, per mouse.
(J) *Prdm1* mRNA expression was determined by qRT-PCR in transduced P14 CD8$^+$ T cells after sorting from spleens 7 days after LCMV infection. Blimp1 protein expression was determined by immunoblot analysis after 4 days of culture with IL-12 (5 ng/ml) and IL-2 (100 U/ml).
(K) Map of *Prdm1* with shRNA-targeted regions indicated.
(L) Contour plots of KLRG-1 and IL-7Rα staining on sh*Prdm1*$^+$ P14 CD8$^+$ T cells from representative mice at 7 days after LCMV infection.
(M) Ratios of memory precursor to effector P14 CD8$^+$ T cells. Each symbol represents T cells from an individual mouse.
Data are pooled from three (H, I) and two (J, L) independent experiments. *$p < 0.05$, **$p < 0.01$, ****$p < 0.0001$. Error bars represent standard deviations.

confirmed that *Prdm1* expression is required for short-lived effector CD8+ T cell differentiation.

Identification of Genes Underlying Tfh Cell Differentiation via an shRNA Screen In Vivo

In parallel, we developed a pooled screen in CD4+ T cells to discover genes important for Tfh and Th1 cell differentiation in vivo (Figure 3A). A total of 5 × 10^5 shRNAmir+Amt^{hi} SMARTA cells were transferred into B6 hosts, and mice were infected 3–4 days later with LCMV Armstrong (Figure 3A). DNA was also isolated from an aliquot of cells before the transfer (input). At 6 days after LCMV infection, virus-specific Tfh cells (CXCR5+ SLAM^{lo}) and Th1 cells (CXCR5−SLAM^{hi}) (Choi et al., 2013; Johnston et al., 2009) were isolated by flow cytometry and deep sequenced for differential representation of the shRNAs. The Tfh:Th1 ratios for each shRNA were calculated and their Z-scores were plotted (Figures 3B and 3C). A total of 14 control shRNAs expected not to affect Tfh or Th1 cell differentiation (not known to be expressed in CD4+ T cells: *Cd14*, *Cd19*, *Cd22*, *Ms4a1*, *Cd8*, *Smarca1*) were equally distributed in both populations (Figure 3B), and their effects on cell accumulation were also assessed (Figure 3C). Based on a Z-score cutoff of $\geq|3.0|$ for each shRNA, factors encoded by *Prdm1*, *Chd4*, *Id2*, and *Ccnt1* were identified as candidate positive regulators of Th1 cells or inhibitors of Tfh cell differentiation (Figures 3B and 3C, Table S1). *Prdm1* is a positive control, as it encodes an inhibitor of Tfh cell differentiation (Johnston et al., 2009), and is discussed further below. Genes *Fosb*, *Plagl1*, *Mta3*, and *Runx3* were identified as potential positive regulators of Tfh cells or inhibitors of Th1 cell differentiation (Table S1). *Plagl1* is highly expressed in Tfh cells (Hale et al., 2013; Yusuf et al., 2010), and MTA3 (encoded by *Mta3*) is known to interact with Bcl6 in B cells (Fujita et al., 2004). Itch is a known positive regulator of Tfh cell differentiation, based on a profound loss of Tfh cells in *Itch*$^{fl/fl}$*Cd4-cre*+ mice (Xiao et al., 2014). Notably, all four *Itch* shRNAs were severely depleted from Tfh cells and highly enriched in the Th1 cell population (Figures 3B and 3C). In a second replicate of the CD4+ T cell screen, the validated *Bcl6* shRNA (sh*Bcl6*.2, Figure S1D) was depleted from the Tfh cell population, as expected (Figure 3D). Comparisons of the two independent screens indicated that the in vivo screens generated reproducible results (Figure 3E) and also showed that shRNA representation was similar even when the libraries were sequenced with increased coverage using the higher-density PGM 318 chip (Figure 3E). These results suggest that the CD4+ T cell shRNAmir-RV screening approach in vivo was also robust.

To confirm results from the primary screen (Figure 3B), the effects of *Prdm1* shRNAs were examined individually. SMARTA CD4+ T cells transduced with sh*Prdm1*.1-RV exhibited the strongest Tfh cell bias in vivo ($p < 0.001$, Figures 3F and 3G), consistent with results from the screen. A modest but significant Tfh cell bias was observed in sh*Prdm1*.3+ and sh*Prdm1*.4+ SMARTA CD4+ T cells when compared to untransduced CD4+ T cells ($p < 0.01$, Figures 3F and 3G). sh*Prdm1*.2 had no effect on Tfh cell differentiation (Figures 3F and 3G), consistent with it having the weakest effect on *Prdm1* mRNA expression in CD4+ T cells (data not shown). These results correlated with the observed distribution of the four shRNAs in the primary screen in CD4+ T cells (Figure 3B) and also indicate that the activity of individual shRNAs might depend on the specific cellular context (e.g., CD4+ versus CD8+ T cells; Figures 3B and 2G). Thus, results of the pooled shRNA screen were consistent with experiments using individual constructs.

Ccnt1 Is Required for Both Th1 Cell and Effector CD8+ T Cell Differentiation In Vivo

We compared the full data sets from the CD8+ and CD4+ T cells screens and found that inhibition of several different genes affected differentiation of both effector CD8+ and CD4+ T cells (Figures 4A and 4B). *Ccnt1* encodes Cyclin T1, a noncanonical cyclin that is a regulatory subunit of the RNA polymerase II-positive transcription elongation factor (P-TEFb). All four *Ccnt1*-specific shRNAs were depleted from KLRG-1^{hi}IL-7Rα^{lo} effector CD8+ T cells and from Th1 cells in the screens (Figure 4A). Based on the notion that functional parallels might exist between differentiation of CD4+ and CD8+ T cells during infection (Choi et al., 2013; Yang et al., 2011), we further explored the roles of Cyclin T1 in both subsets.

In CD4+ T cells, all four *Ccnt1*-shRNAs inhibited Cyclin T1 protein expression to varying degrees; three of four caused robust inhibition (Figures 4C and S6A). Each *Ccnt1* shRNA was examined individually in SMARTA CD4+ T cells 6 days after LCMV infection (Figures 4D–4G). Neither CD4+ T cell proliferation (Figures S6B and S6C) nor CD4 or CD44 expression was affected by *Ccnt1* shRNAs (data not shown). *Ccnt1* shRNAs both increased Tfh cell development (CXCR5+SLAM^{lo}) and decreased Th1 cell formation ($p < 0.0001$–0.05; Figures 4D and 4E). Germinal center Tfh (GC Tfh) cells are a fully polarized subset of Tfh cells (CXCR5+PSGL1^{lo}; Crotty, 2011; Poholek et al., 2010) and their frequencies were increased by *Ccnt1* shRNAs ($p < 0.001$–0.05; Figures 4F and 4G).

We also examined T cell differentiation at earlier times points and found that *Ccnt1* shRNAs substantially increased the proportion of early CXCR5+Bcl6+ Tfh cells ($p < 0.01$; Figures 4H and 4I, and $p < 0.01$–0.05; Figure S6D). The increased Tfh cell differentiation of sh*Ccnt1*+CD4+ T cells after LCMV infection could be a reflection of a decreased potential of these cells to differentiate into Th1 cells. Consistent with this hypothesis, *Ccnt1* shRNAs resulted in decreased expression of T-bet in vivo ($p < 0.001$–0.05; Figure 4J). Reciprocally, the expression of CD40L, an essential component of T cell help to B cells, was also increased in sh*Ccnt1*+ cells ($p < 0.001$–0.05; Figure 4K). These results suggest that Cyclin T1 promotes Th1 cell differentiation at the expense of Tfh cell differentiation in vivo.

To test the requirement for Cyclin T1 in T cell differentiation in vitro, we cultured sh*Con*+ and sh*Ccnt1*+ CD4+ T cells in Th1-cell-biasing conditions. *Ccnt1* shRNAs impaired T-bet expression under these conditions ($p < 0.0001$; Figure 5A), resulting in a substantial loss of IFN-γ production upon restimulation ($p < 0.0001$–0.001; Figures 5B and 5C). The defect was cell intrinsic, because no defect in IFN-γ production was observed in untransduced CD4+ T cells in the same wells (Figure S6E). These results support a model in which reduced Cyclin T1 expression impairs Th1 cell development and favors Tfh cell development.

The P-TEFb Subunit Cdk9 Is Necessary for Th1 Cell Differentiation

Conventional P-TEFb comprises Cdk9 (catalytic subunit) and a regulatory subunit (e.g., Cyclin T1 or T2). To test whether Cyclin

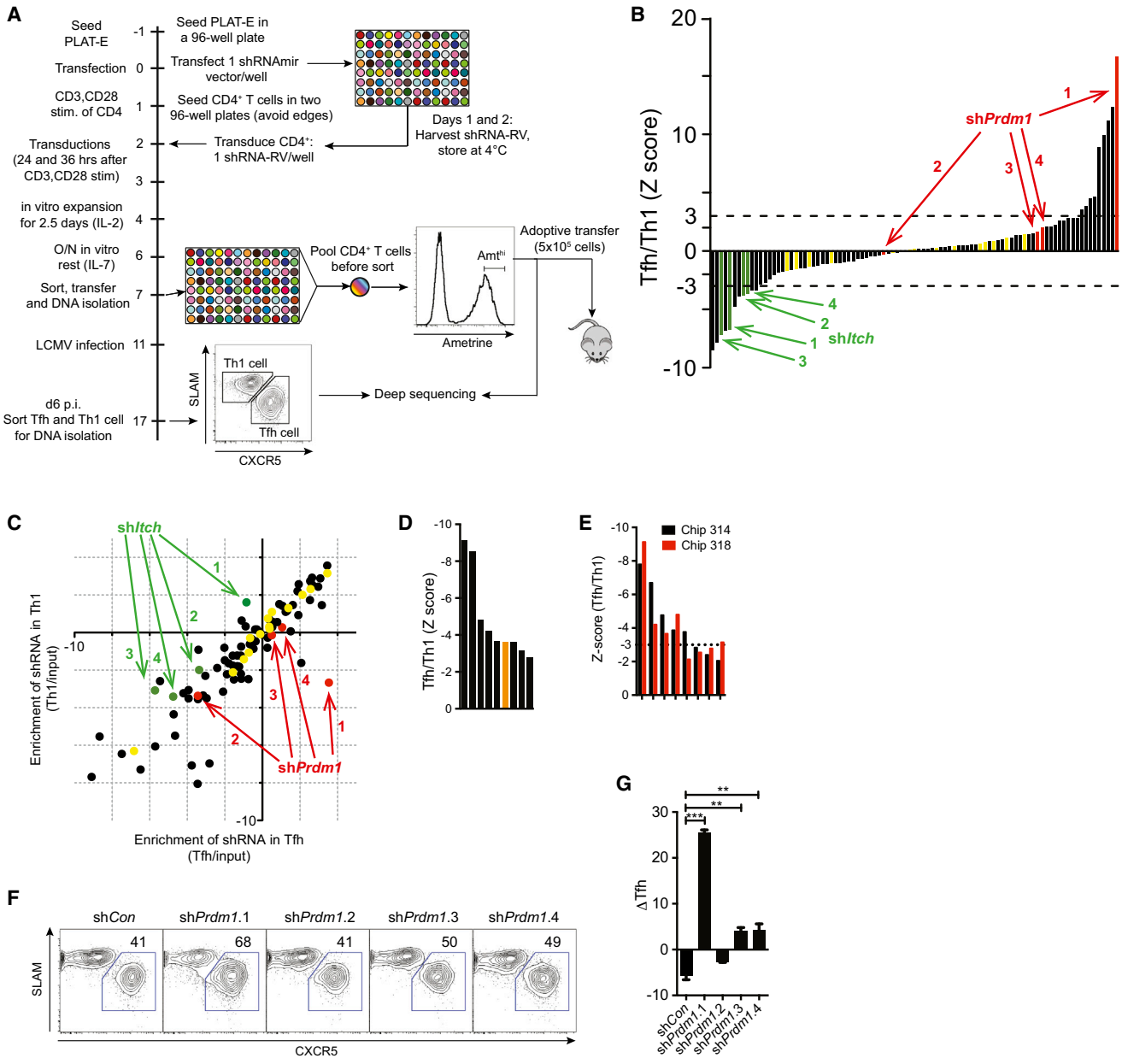

Figure 3. A Pooled RNAi Screen in CD4+ T Cells Identifies Potential Regulators of Tfh and Th1 Cell Differentiation In Vivo

(A) Scheme for the shRNAmir screening approach using SMARTA CD4+ T cells.

(B) Relative enrichment of shRNAs in the Tfh or Th1 cell populations in vivo, reported as Z-score values for each shRNA in the library. Z-scores of |3| and |2| are indicated by a dotted line and a tick, respectively.

(C) Scatter plot shows the $\log_2$ of normalized reads of all shRNA in Tfh and Th1 cell populations versus the input sample. This reveals effects on cell survival or proliferation. shRNA are color coded as in (B).

(D) Z-scores are shown for the shRNAs most depleted from the Tfh cell population in the Ion 318 Chip experiment. sh*Bcl6* is highlighted in orange.

(E) Z-scores of shRNAs depleted from Tfh cells in two independent deep sequencing reactions: Ion 314 Chip (black bars) and Ion 318 Chip (red bars). The dotted line is a Z-score of −3.

(F) SMARTA CD4+ T cells were transduced with the indicated shRNAs, transferred into B6 mice, and analyzed 6 days after LCMV infection. shCon indicates a control shRNAmir. Representative flow cytometry plots are shown of shRNA+ SMARTA CD4+ T cells with Tfh cell ($CXCR5^+SLAM^{lo}$) gate drawn.

(G) The differences in percentages of Tfh (%Tfh of Amt^+ − %Tfh of Amt^-) for each shRNAmir in SMARTA CD4+ T cells are shown. **p < 0.01, ***p < 0.001. Error bars represent standard deviations.

T1 was likely acting via P-TEFb, we examined two *Cdk9* shRNAs in SMARTA CD4+ T cells for their effects on Tfh versus Th1 cell differentiation. Both shRNAs inhibited *Cdk9* expression in vitro (Figure 5D). CD4+ T cells transduced with *Cdk9* shRNAs and cultured under Th1-cell-biasing conditions showed impaired production of IFN-γ, similar to the effect of *Ccnt1*

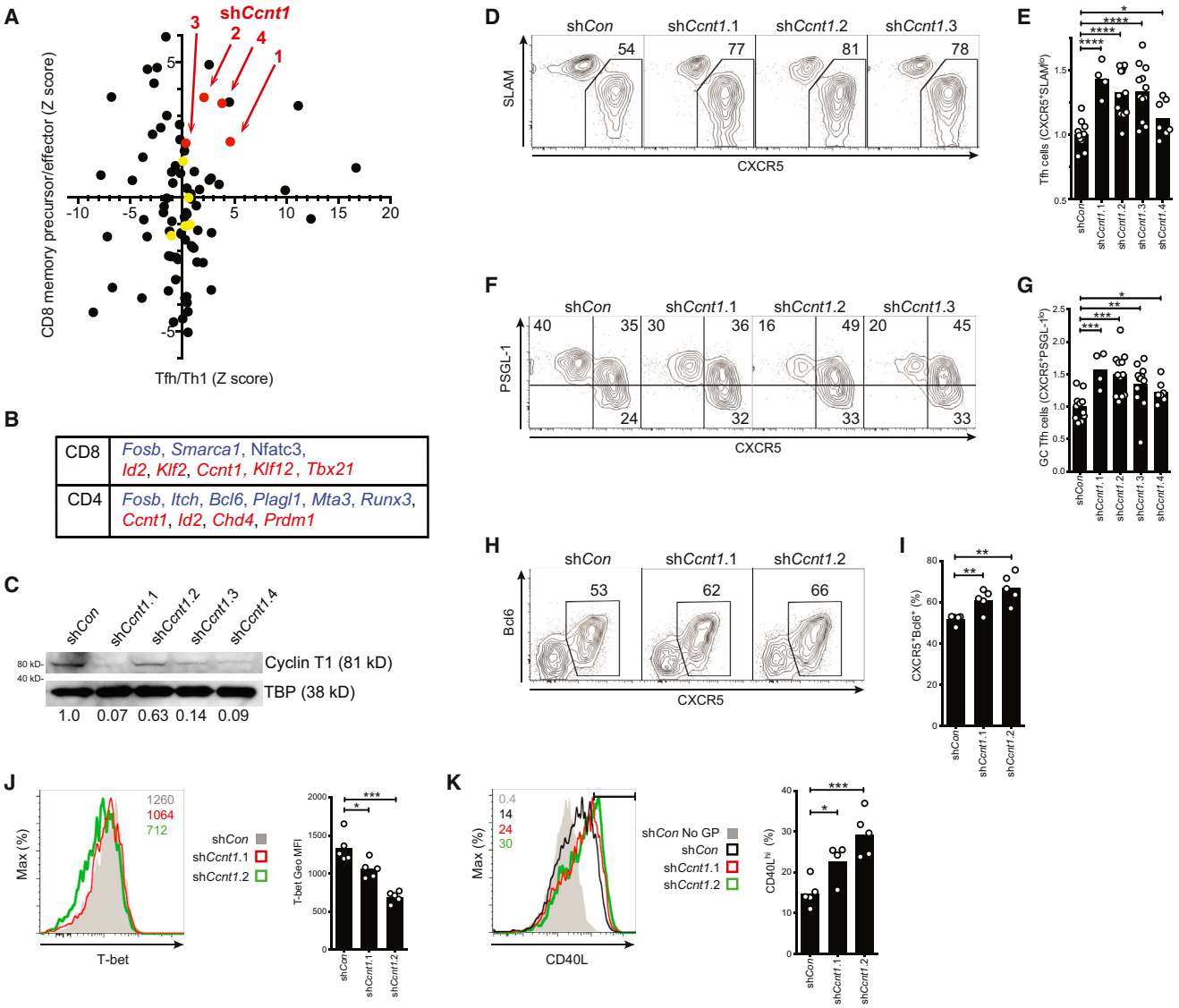

Figure 4. *Ccnt1* Depletion Promotes Development of Tfh Cells during Viral Infection

(A) Comparison of shRNAmir screening results in both CD4$^+$ and CD8$^+$ T cells. Tfh and Th1 CD4$^+$ T cells differentiation results, plotted against memory precursor and effector CD8$^+$ T cell differentiation results. Z-score values are shown. Common negative control shRNAs are shown in yellow, and those targeting *Ccnt1* are highlighted (red).

(B) Table of top hits for genes required for memory precursor CD8$^+$ T cell or Tfh CD4$^+$ T cell differentiation (blue) and short-lived effector CD8$^+$ T cell or Th1 CD4$^+$ T cell differentiation (red).

(C) Cyclin T1 protein expression in MCC T cells after transduction with the indicated shRNAs and 4 days of culture. The ratios of Cyclin T1 to TBP relative to the control shRNA are indicated.

(D and E) Flow cytometry plots (D) and quantitation (normalized) (E) of Tfh cell differentiation (CXCR5$^+$SLAM^{lo}) by sh*Ccnt1*$^+$ SMARTA CD4$^+$ T cells at 6 days after LCMV infection.

(F and G) Flow cytometry plots (F) and quantitation (normalized) (G) of GC Tfh cell differentiation (CXCR5$^+$PSGL1^{lo}) by sh*Ccnt1*$^+$ SMARTA CD4$^+$ T cells at 6 days after LCMV infection.

(H and I) Flow cytometry plots (H) and quantitation (I) of CXCR5 and Bcl6 expression by sh*Ccnt1*$^+$ SMARTA CD4$^+$ T cells at 4 days after LCMV infection.

(J) T-bet expression in sh*Ccnt1*$^+$ SMARTA CD4$^+$ T cells in vivo, 3 days after LCMV infection. T-bet geometric MFIs are graphed (right).

(K) CD40L expression by sh*Ccnt1*$^+$ SMARTA CD4$^+$ T cells at 4 days after LCMV infection, after 2 hr restimulation with GP_{61-80} peptide. The percentages of CD40L^{hi} cells are indicated. Each symbol represents T cells from an individual mouse.

Data are pooled from three (F, G) or representative of two (K) or three (H–J) independent experiments. *p < 0.05, **p < 0.01, ***p < 0.001, ****p < 0.0001.

shRNAs (p < 0.001–0.01; Figures 5E and 5F), suggesting that both Cyclin T1 and Cdk9 promote Th1 cell differentiation in vitro.

Cdk9 depletion in vivo favored Tfh (CXCR5$^+$SLAM^{lo}) cell development while reducing Th1 cell differentiation (sh*Cdk9*.1, p < 0.0001; Figures 5G and 5H), without impairing T cell expansion

(Figure S7A) or normal expression of CD4 and CD44. Furthermore, Cdk9 depletion increased the frequency of GC Tfh cells, measured as $CXCR5^+PSGL1^{lo}$ cells (sh*Cdk9*.1, $p < 0.001$; Figures 5I and 5J) or $CXCR5^+Bcl6^{hi}$ cells (Figures S7B and S7C). Additionally, based on CXCR5 and Bcl6 expression, early Tfh cell differentiation in sh$Cdk9^+CD4^+$ T cells was enhanced 4 days after LCMV infection ($p < 0.01$–0.05; Figures 5K and 5L), with normal cell expansion (Figure S7D). Intriguingly, similar to what was observed in the absence of Cyclin T1, inhibition of *Cdk9* expression also increased CD40L expression by $CD4^+$ T cells ($p < 0.001$–0.01; Figure 5M). Altogether, these data recapitulated those obtained with sh$Ccnt1^+CD4^+$ T cells and suggest that P-TEFb might preferentially promote Th1 cell differentiation of activated $CD4^+$ T cells.

Ccnt1 and *Cdk9* Are Required for Development of Protective Effector CTLs In Vivo

Next, we explored the requirements of *Ccnt1* expression in $CD8^+$ T cells. Three of the four *Ccnt1*-specific shRNAs resulted in near complete inhibition of Cyclin T1 protein expression in cultured $CD8^+$ T cells; one shRNA exhibited strong but incomplete inhibition (Figure 6A). The accumulation of P14 $CD8^+$ T cells transduced with *Ccnt1* shRNAs was not impaired during culture (Figure 6B) or in vivo (Figure 6C). However, *Ccnt1* shRNAs strongly impaired generation of short-lived effector P14 T cells (Figures 6D and 6E). There was a concomitant increase in the fraction of memory precursor phenotype P14 cells (Figures 6D and 6F), which increased the ratio of memory precursor to short-lived effector P14 cells (Figure 6G).

To examine whether the effects of *Ccnt1* shRNAs in $CD8^+$ T cells were related to Cyclin T1 function as a subunit of P-TEFb, we examined the effects of *Cdk9*-specific shRNAs (Figure 6H). Similar to sh*Ccnt1*, sh$Cdk9^+$ P14 cells exhibited reduced short-lived effector cell and increased memory precursor cell formation in vivo (Figures 6I–6K). This correlated with decreased T-bet expression in vivo (Figure 6L). Notably, T-bet expression in sh$Ccnt1^+$ or sh$Cdk9^+$ P14 cells was impaired in KLRG-1^{lo}IL-$7R\alpha^{lo}$ cells (data not shown), a stage that presumably precedes development of either short-lived effector or memory precursor $CD8^+$ T cells. These data show that wild-type amounts of Cyclin T1 and Cdk9 are necessary for efficient development of short-lived effector CTLs and that they normally limit generation of memory precursor $CD8^+$ T cells.

The defect in sh$Ccnt1^+$ and sh$Cdk9^+$ short-lived effector $CD8^+$ T cell formation brought into question whether these cells were effective at viral control. Thus, we examined LCMV burden on day 8 of infection. LCMV titers in the spleen of host mice with sh$Ccnt1^+$ or sh$Cdk9^+$ P14 cells were at least 2- to 5-fold higher than controls (Figure 7A). Correlating with this finding, sh$Ccnt1^+$ or sh$Cdk9^+$ P14 cells from infected mice expressed less granzyme B (Figure 7B). Finally, we examined sh$Ccnt1^+$ or sh$Cdk9^+$ P14 cells under culture conditions that strongly induce CTL differentiation (Pipkin et al., 2010). Under these conditions, all shRNAs targeting either *Ccnt1* or *Cdk9* also specifically inhibited perforin protein expression (Figure 7C). Thus, normal amounts of Cyclin T1 and Cdk9 appear to be required for the upregulation of genes encoding cytotoxic effector functions and for effective CTL-mediated protection from viral infection.

DISCUSSION

We have demonstrated the applicability of a pooled approach using shRNAmirs in T cells to screen for factors that regulate $CD4^+$ and $CD8^+$ T cell differentiation in response to viral infection. Using an improved shRNAmir vector that enhances suitability of shRNA-mediated RNAi in studies that depend upon cell transfers, more than 100 unique shRNAs were screened simultaneously in vivo. In separate proof-of-principle screens during LCMV infection using virus-specific TCR transgenic SMARTA $CD4^+$ T cells or P14 $CD8^+$ T cells, we identified multiple candidate genes with potential roles in the development of Th1 and Tfh $CD4^+$ T cells as well as short-lived effector and memory precursor $CD8^+$ T cells. Detailed follow-up analyses of one factor identified in both screens revealed specific roles for Cyclin T1 and Cdk9, components of P-TEFb, for promoting Th1 cell development of $CD4^+$ T cells and protective effector CTL development of $CD8^+$ T cells during infection, while limiting differentiation of Tfh cells and memory precursor $CD8^+$ T cells. These data suggest that regulation of transcription elongation by P-TEFb might be an important mechanism underpinning differentiation of T cells during immune responses.

Several important aspects distinguish the screen presented here from other recently reported pooled in vivo shRNA-screens (Beronja et al., 2013; Zhou et al., 2014; Zuber et al., 2011). The screening approach here used an array strategy to ensure independent transductions and equal representation of shRNAmirs in the input pools. In addition, in contrast to other screens based on shRNA-dependent cell accumulation or depletion as the main readout to identify primary hits (Beronja et al., 2013; Zhou et al., 2014; Zuber et al., 2011), the approach presented here was a phenotypic screen of cell differentiation during an infection. As such, it was complicated by the nature of T cell responses during infection, which are constrained by factors such as the frequencies of antigen-specific T cells (Badovinac et al., 2007; Obar et al., 2008), and thus, is distinct from a T cell adoptive immunotherapy setting, which affords transferring much larger T cell numbers (Zhou et al., 2014).

The ability to conduct large-scale pooled screens using shRNAs has advanced, although interpreting the results of shRNA-based assays remains complicated. As our data on the *Prdm1*, *Tbx21*, and *Ccnt1* genes emphasize, interrogating the effects of multiple shRNAs targeting the same gene in several assays tends to clarify the role of each gene, because each shRNA can result in nonidentical phenotypes attributable to differential effects on particular target RNA isoforms, unintended off-target effects, or partial attenuation of target-specific gene expression. In our experience, ~60% of shRNA sequences derived from the GIPZ library (the source of most shRNAs for this study) impaired target gene expression or caused a measurable biological phenotype (data not shown). However, newer algorithms trained on functional data have improved predicting shRNAmirs that trigger RNAi more potently and specifically than previous designs (Fellmann et al., 2011). Our study employed some of these designs and they are likely to enhance the fidelity of future large-scale screens in vivo.

Using a conservative approach, we showed that more than 100 unique shRNAmirs represented by 500,000 adoptively transferred P14 cells could be assayed in fewer than 10 mice in

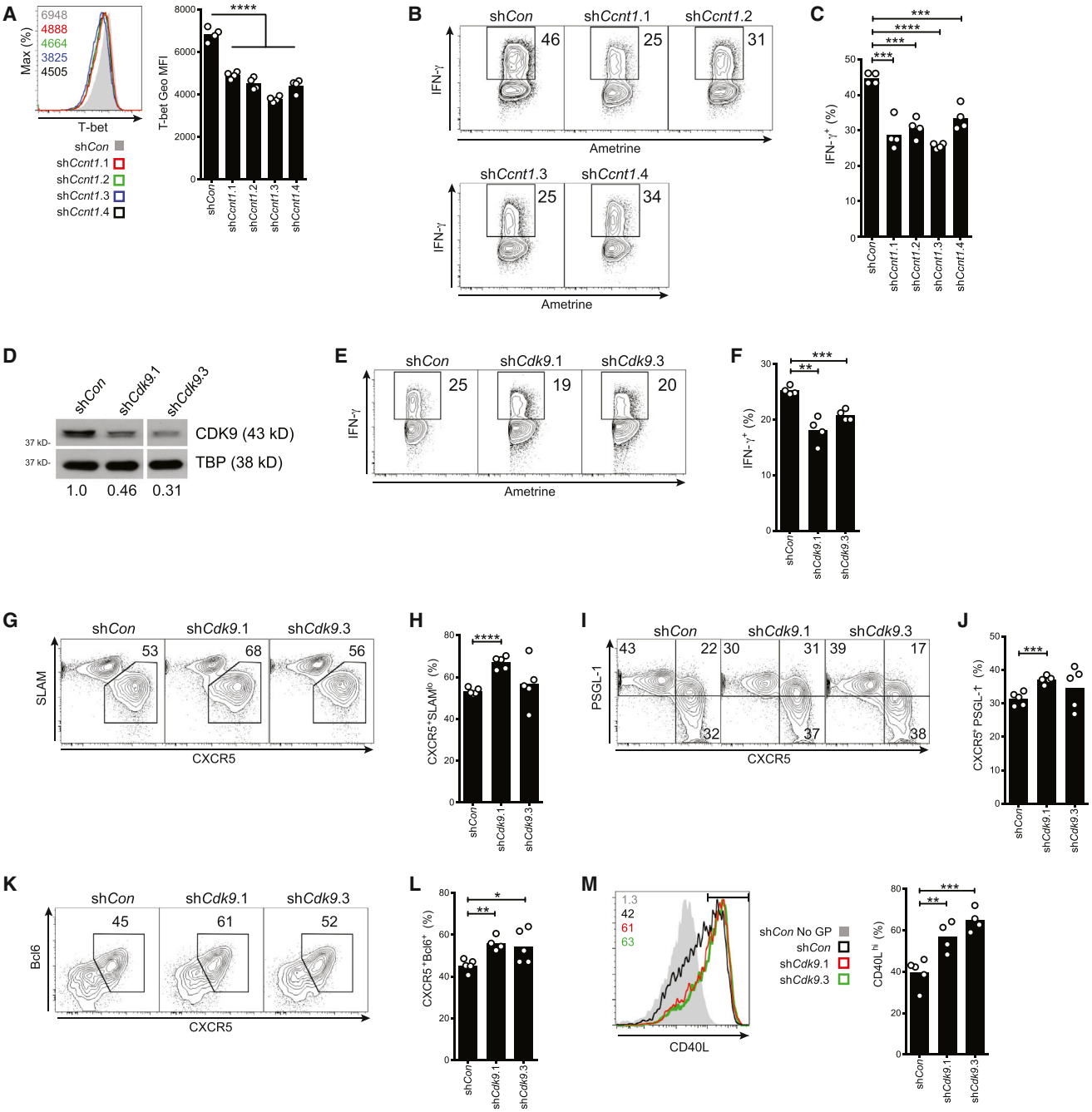

Figure 5. Cyclin T1 and Cdk9 Depletion Impairs Th1 Cell Differentiation In Vitro and In Vivo

(A–C, E, and F) CD4+ T cells were transduced with *Ccnt1* shRNAs and cultured under Th1-cell-biasing conditions for 4 days before restimulation with PMA and ionomycin for 1 (E and F) or 4 (A–C) hr.

(A) T-bet expression by sh*Ccnt1*+ CD4+ T cells. Quantitation and an example histogram are shown.

(B) Flow cytometry plots of IFN-γ expression by sh*Ccnt1*+ CD4+ T cells upon restimulation.

(C) Quantitation of (B), for all samples.

(D) Cdk9 protein expression in sh*Cdk9*+ MCC T cells.

(E) Flow cytometry plots of IFN-γ expression by sh*Cdk9*+CD4+ T cells upon restimulation.

(F) Quantitation of (E), for all samples.

(G and H) Flow cytometry plots (G) and quantitation (H) of Tfh cell differentiation (CXCR5+SLAMlo) by sh*Cdk9*+ SMARTA CD4+ T cells at 6 days after LCMV infection.

(I and J) Flow cytometry plots (I) and quantitation (J) of GC Tfh cell differentiation (CXCR5+PSGL1lo) by sh*Cdk9*+ SMARTA CD4+ T cells at 6 days after LCMV infection.

(legend continued on next page)

approximately 1 week. Under these conditions, we estimated that each shRNA was represented ~500 times per mouse after T cell engraftment, which is ~10-fold higher representation of each shRNA than a recent pooled screen that examined skin cell development in vivo (Beronja et al., 2013; Zuber et al., 2011) and involved transferring 10-fold fewer T cells than a recent immunotherapy screen in T cells (Zhou et al., 2014). Taking these studies into account with our results, we anticipate that by using our system and applying deeper sequencing, it is likely to be feasible to perform phenotypic screens on pools of 1,000 or more shRNAs in parallel in T cells during infection.

The screen discovered unanticipated roles for Cyclin T1 and Cdk9 in the regulation of T cell differentiation during antiviral immune responses and emphasizes the specificity that ubiquitously expressed factors can have. Cyclin T1 and Cdk9 are two widely expressed components of P-TEFb (Oven et al., 2007; Peterlin and Price, 2006), which stimulates the transition of paused RNA polymerase II complexes into productive elongation (Peterlin and Price, 2006). The regulation of transcription elongation might govern a substantial fraction of differential expression of transcriptionally active genes (Min et al., 2011; Peterlin and Price, 2006; Rahl et al., 2010), and it is notable that this process is also critical in the regulation of HIV transcription in CD4+ T cells. The fact that depletion of Cyclin T1 or Cdk9 in activated T cells results in specific alterations in their differentiation in vitro and in vivo indicates that these factors are utilized in context-specific regulation of gene expression in T cells, despite their ubiquitous expression. Indeed, ChIP-seq analysis showed that Cyclin T1 is specifically recruited to subsets of genes, including *Tbx21*, *Prf1*, *Ifng*, and *Il2ra*, that are activated in response to TCR-like stimulation of CD8+ T cells (M.E.P., unpublished data).

Given the known functions of Cyclin T1 and Cdk9 in P-TEFb, one interpretation of our results is that T cell differentiation is regulated via transcriptional elongation by P-TEFb. However, the phenotypes upon Cyclin T1 and Cdk9 depletion were not identical, although they were similar. One simple explanation of this outcome is that shRNA-mediated depletion of Cdk9 was less efficient than for Cyclin T1, resulting in different amounts of functional P-TEFb in each case. Another interpretation is alternative factors that "compensate" for reductions in wild-type Cyclin T1 or Cdk9 amounts, and which possess distinct activities or targeting, caused the observed phenotypes. Indeed, other Cyclins and Cyclin-dependent kinases can phosphorylate the C-terminal domain of RNA Pol II at serine 2 and regulate transcription, and could be cell type specific (Blazek et al., 2011). Finally, Cyclin T1 and Cdk9 could have roles in T cells apart from their established roles in P-TEFb. Future studies to elucidate the specific roles of Cyclin T1 and Cdk9 and how they integrate with the external signals that govern CD4+ and CD8+ T cell differentiation are likely to open previously unappreciated insights into T cell function. In summary, the functional genetic approach described here is likely to facilitate the identification of many previously unknown players.

EXPERIMENTAL PROCEDURES

Animals and Viruses

C57BL/6 (B6) mice were purchased from the Jackson Laboratory. CD45.1+ SMARTA (SM; lymphocytic choriomeningitis virus [LCMV] gp66-77-IA^b specific) (Oxenius et al., 1998) and Blimp1-YFP mice were bred in-house. LCMV gp33-41-specific P14 Thy1.1+ mice used for in vivo analysis were a gift from R. Ahmed (Emory University); P14 *Tcra*$^{-/-}$ mice were used for in vitro studies (Taconic). All mice were maintained in specific-pathogen-free facilities and used according to protocols approved by the animal care and use committees of the LIAI and TSRI-FL. Virus stocks were made as described (Johnston et al., 2009), and LCMV titers in tissues were assessed by plaque assay.

Pooled Screening Approaches

Please refer to Supplemental Experimental Procedures.

Flow Cytometry

Single-cell suspensions of spleens were prepared by mechanical disruption. Surface staining for flow cytometry was performed by standard techniques (Johnston et al., 2009) and the following clones: CD4 (RM4-5), CD45.1 (A20), CD44 (IM7), and CD62L (MEL-14) (eBiosciences); CD8 (53-6.7) and B220 (RA3-6B2) (BD Biosciences); as well as CD8 (53-6.7), CD127 (A7R34), KLRG-1 (2F1), CD90.1 (OX-7), and SLAM (TC15-12F12.2) (BioLegend). CXCR5 staining was performed as described (Choi et al., 2013). Intracellular staining after surface stains was performed using the "Foxp3 staining buffer" set (eBiosciences), using anti-Bcl6 monoclonal antibody (K112-91, BD Biosciences), anti-Tbet (4B10), or anti-Granzyme B (GB11) (Biolegend).

Adoptive Transfer Analysis of Individual shRNAmirs in CD8+ or CD4+ T Cells

For in vivo confirmation of "hits," SMARTA CD4+ or P14 CD8+ T cells were transduced with viral supernatants generated from individual shRNAmir-RV constructs (Supplemental Experimental Procedures). A total of 5 × 10^5 P14 cells were transferred into 6-week-old B6 mice 1 or 2 days after activation and analyzed on day 7 or 8 after infection. Note, transfer of P14 cells on day 1 rather than day 2 after activation was found to recapitulate differentiation more physiologically (data not shown). For CD4+ T cell experiments, 25,000 SMARTA cells were transferred.

RNA and Protein Analysis

Total RNA was isolated from transduced (Ametrine+) CD4+ or CD8+ T cells and used for cDNA synthesis as previously described (Johnston et al., 2009). qPCR reactions were performed in triplicate using the SYBR Select Master Mix (Life Technologies) on a Roche Lightcycler 480, using primers specific to *Prdm1* (F-5′-TTCTCTTGGAAAAACGTGTGGG-3′; R-5′-GGAGCCGGAG CTAGACTTG-3′) and *Tbx21* (F-5′-ACCAACAACAAGGGGGCTTC-3′; R-5′-CTCTGGCTCTCCATCATTCACC-3′). For immunoblot analysis, whole-cell lysates were obtained from CD8+ T cells on day 6 after activation, from CD4+ T cells 5 days after activation, or from MCC-T cells by sorting transduced (Ametrine+) cells and lysis in 150 mM NaCl, 25 mM Tris (pH 7.5), 1% Triton X-100, 0.1% SDS, 0.5% Deoxycholate, and complete protease inhibitors (Roche). 25 μg of protein was resolved by 8% SDS-PAGE, transferred to nitrocellulose membranes, and probed with anti-Cyclin T1 (sc-10750), anti-Blimp1 (sc-47732), anti-Cdk9 (sc-484) (Santa Cruz Biotechnology), anti-Perforin (ab16074), and anti-beta Actin (Abcam ab8227).

SUPPLEMENTAL INFORMATION

Supplemental Information includes seven figures, one table, and Supplemental Experimental Procedures and can be found with this article online at http://dx.doi.org/10.1016/j.immuni.2014.08.002.

(K and L) Flow cytometry plots (K) and quantitation (L) of CXCR5 and Bcl6 expression by sh*Cdk9*+ SMARTA CD4+ T cells, 4 days after LCMV infection.
(M) Histograms of CD40L expression on sh*Cdk9*+ SMARTA CD4+ T cells, after isolation from spleens 4 days after LCMV infection and restimulation with GP_{61-80} peptide for 4 hr. The percentages of CD40L^{hi} SMARTA are shown and summarized (right).
Data are representative of two independent experiments. *p < 0.05, **p < 0.01, ***p < 0.001, ****p < 0.0001.

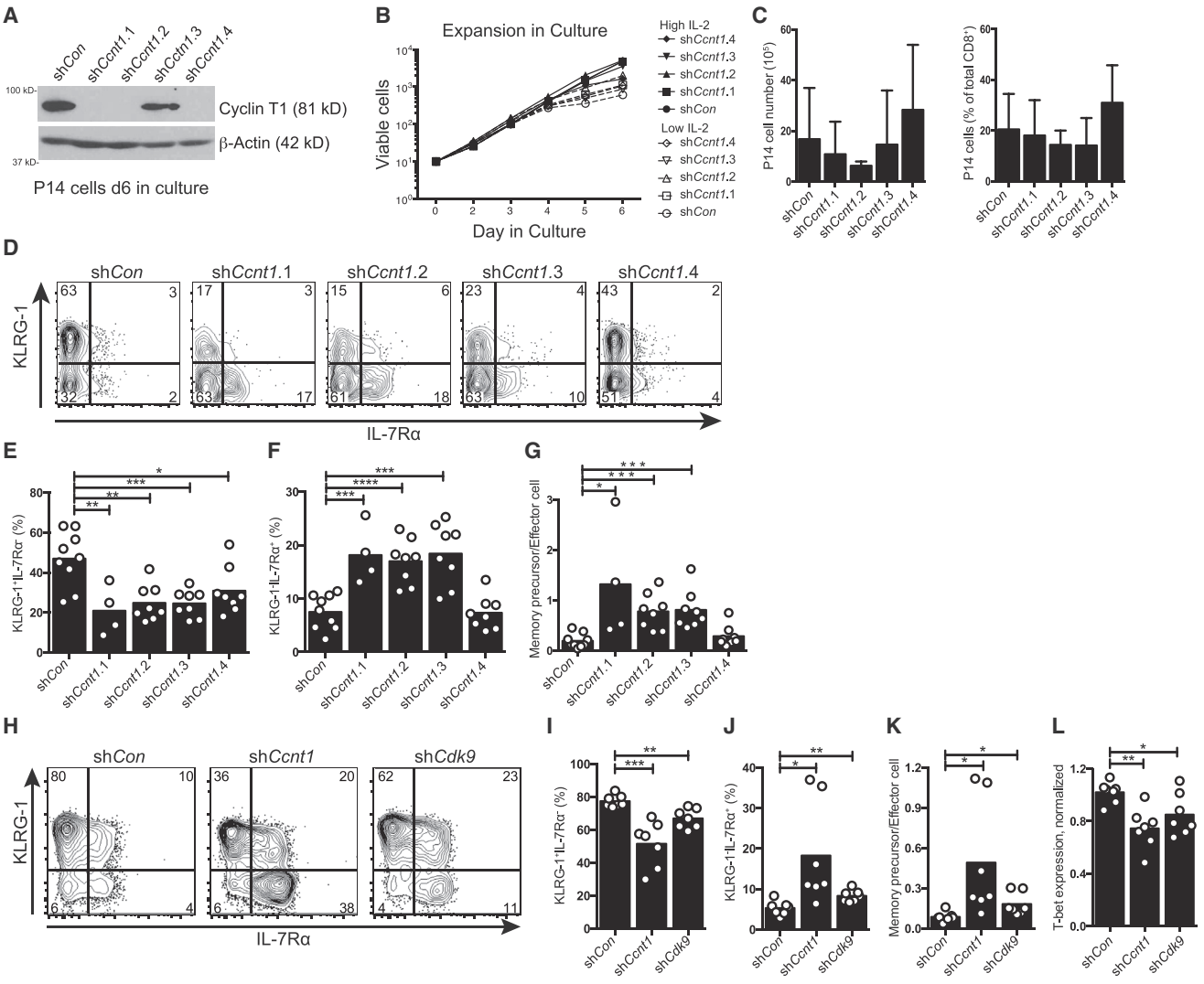

Figure 6. Cyclin T1 and Cdk9 Depletion Impairs Generation of Effector CD8⁺ T Cells during LCMV Infection

(A) Immunoblot analysis of Cyclin T1 in FACS-sorted sh*Ccnt1*⁺ P14 CD8⁺ T cells. Cells were cultured 6 days in low IL-2 (10 U/ml).

(B) Expansion of FACS-sorted sh*Ccnt1*⁺ P14 CD8⁺ T cells in culture. Low IL-2 (10 U/ml), high IL-2 (100 U/ml).

(C–L) Adoptively transferred P14 CD8⁺ T cells transduced with the indicated shRNAs were analyzed on day 7 (C–G) or day 8 (H–L) after LCMV infection.

(C) The numbers and percentages of sh*Ccnt1*⁺ P14 cells in the spleen.

(D) Contour plots show KLRG-1 and IL-7Rα staining on sh*Ccnt1*⁺ P14 CD8⁺ T cells from representative mice 7 days after LCMV infection.

(E–G) Quantitation of CD8⁺ T cell subsets from sh*Ccnt1*⁺ P14 cells in vivo.

(E) Short-lived effector cells (KLRG-1^{hi}IL-7Rα^{lo}).

(F) Memory precursor cells (KLRG-1^{lo}IL-7Rα^{hi}).

(G) Ratio of memory precursor to short-lived effector phenotype P14 cells, per mouse.

(H) Contour plots show KLRG-1 and IL-7Rα staining by sh*Cdk9*⁺ P14 CD8⁺ T cells from representative mice 8 days after LCMV infection.

(I–L) Quantitation of CD8⁺ T cell subsets from sh*Cdk9*⁺ P14 cells in vivo.

(I) Short-lived effector cells (KLRG-1^{hi}IL-7Rα^{lo}).

(J) Memory precursor cells (KLRG-1^{lo}IL-7Rα^{hi}).

(K) Ratio of memory precursor to short-lived effector phenotype P14 cells, per mouse.

(L) Summarized T-bet expression based on intracellular staining and flow cytometry.

Each symbol represents T cells from separate mice. Data are pooled from two independent experiments. *$p < 0.05$, **$p < 0.01$, ***$p < 0.001$, ****$p < 0.0001$. Error bars represent standard deviations.

AUTHOR CONTRIBUTIONS

R.C. established the pooled approaches, implemented and analyzed the CD8⁺ T cell screen and follow-up, and assisted writing the paper. S.B. designed, implemented, and analyzed the CD4⁺ T cell screen and follow-up, and assisted writing the paper. M.A.F. performed CD8⁺ T cell follow-up analysis. B.L. designed the sequencing bioinformatic pipeline. R.J.J. designed vectors and did preliminary experiments. S.S., N.X., and Y.-C.L. provided reagents and advice. A.R. assisted with experimental design, provided resources, and assisted writing the paper. B.P. designed the sequencing

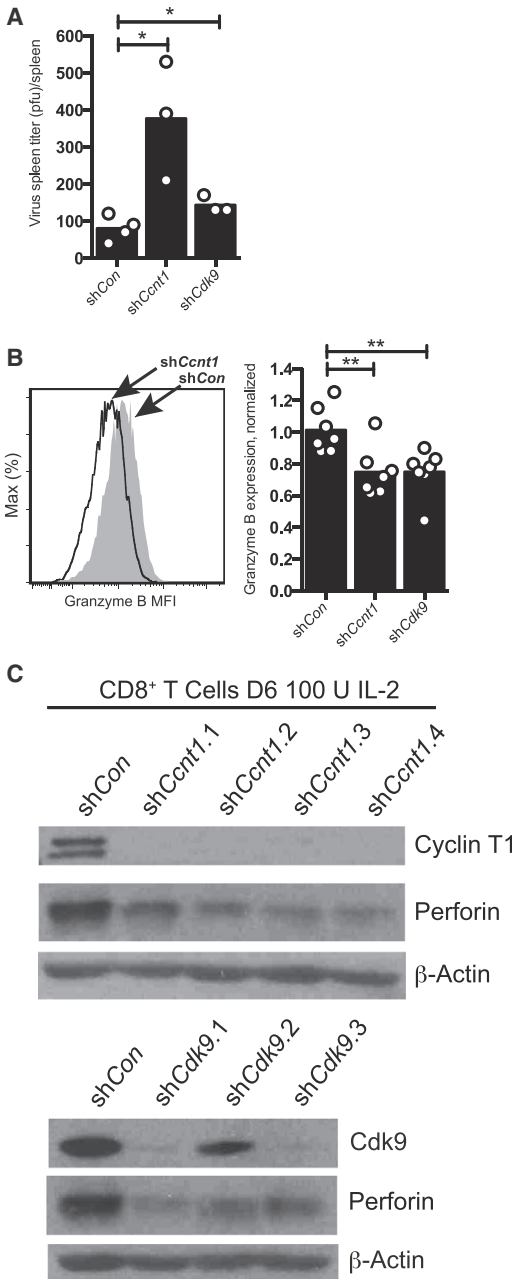

Figure 7. Cyclin T1 and Cdk9 Are Required for Antiviral CTL Functions

(A) LCMV titers in spleen were determined 8 days after LCMV infection.

(B) Granzyme B expression in P14 cells at day 8 postinfection. Histogram (left) and quantitation (geometric MFI; right).

(C) Immunoblot analysis of Cyclin T1, Cdk9, Perforin, and β-actin expression in whole-cell lysates from flow cytometry-sorted sh*Ccnt1*+ and sh*Cdk9*+ P14 CD8+ T cells after 6 days in culture (100 U/ml).

analysis pipeline and supervised statistical analyses. M.E.P. and S.C. conceived of the studies, designed experiments, analyzed data, supervised the projects, and wrote the paper.

ACKNOWLEDGMENTS

This work was supported by NIH grants RC4 AI092763 to M.E.P., R.C., S.S., B.P., and A.R.; NIH R01 AI095634 to M.E.P.; NIH R01 CA42471 to A.R.; NIH R01 072543 to S.C.; NIH U19 AI109976 to S.C. and M.E.P.; Frenchmen's Creek Women for Cancer Research to R.C.; and a Postdoctoral Training Award from the Fonds de la recherche santé Québec to S.B. We thank G. Martinez for advice and assistance.

Received: November 8, 2013
Accepted: August 4, 2014
Published: August 21, 2014

REFERENCES

Araki, K., Turner, A.P., Shaffer, V.O., Gangappa, S., Keller, S.A., Bachmann, M.F., Larsen, C.P., and Ahmed, R. (2009). mTOR regulates memory CD8 T-cell differentiation. Nature *460*, 108–112.

Badovinac, V.P., Haring, J.S., and Harty, J.T. (2007). Initial T cell receptor transgenic cell precursor frequency dictates critical aspects of the CD8(+) T cell response to infection. Immunity *26*, 827–841.

Beronja, S., Janki, P., Heller, E., Lien, W.H., Keyes, B.E., Oshimori, N., and Fuchs, E. (2013). RNAi screens in mice identify physiological regulators of oncogenic growth. Nature *501*, 185–190.

Best, J.A., Blair, D.A., Knell, J., Yang, E., Mayya, V., Doedens, A., Dustin, M.L., and Goldrath, A.W.; Immunological Genome Project Consortium (2013). Transcriptional insights into the CD8(+) T cell response to infection and memory T cell formation. Nat. Immunol. *14*, 404–412.

Blazek, D., Kohoutek, J., Bartholomeeusen, K., Johansen, E., Hulinkova, P., Luo, Z., Cimermancic, P., Ule, J., and Peterlin, B.M. (2011). The Cyclin K/Cdk12 complex maintains genomic stability via regulation of expression of DNA damage response genes. Genes Dev. *25*, 2158–2172.

Cannarile, M.A., Lind, N.A., Rivera, R., Sheridan, A.D., Camfield, K.A., Wu, B.B., Cheung, K.P., Ding, Z., and Goldrath, A.W. (2006). Transcriptional regulator Id2 mediates CD8+ T cell immunity. Nat. Immunol. *7*, 1317–1325.

Chang, J.T., Palanivel, V.R., Kinjyo, I., Schambach, F., Intlekofer, A.M., Banerjee, A., Longworth, S.A., Vinup, K.E., Mrass, P., Oliaro, J., et al. (2007). Asymmetric T lymphocyte division in the initiation of adaptive immune responses. Science *315*, 1687–1691.

Choi, Y.S., Yang, J.A., Yusuf, I., Johnston, R.J., Greenbaum, J., Peters, B., and Crotty, S. (2013). Bcl6 expressing follicular helper CD4 T cells are fate committed early and have the capacity to form memory. J. Immunol. *190*, 4014–4026.

Ciofani, M., Madar, A., Galan, C., Sellars, M., Mace, K., Pauli, F., Agarwal, A., Huang, W., Parkurst, C.N., Muratet, M., et al. (2012). A validated regulatory network for Th17 cell specification. Cell *151*, 289–303.

Crotty, S. (2011). Follicular helper CD4 T cells (TFH). Annu. Rev. Immunol. *29*, 621–663.

Crotty, S. (2012). The 1-1-1 fallacy. Immunol. Rev. *247*, 133–142.

Doering, T.A., Crawford, A., Angelosanto, J.M., Paley, M.A., Ziegler, C.G., and Wherry, E.J. (2012). Network analysis reveals centrally connected genes and pathways involved in CD8+ T cell exhaustion versus memory. Immunity *37*, 1130–1144.

Fellmann, C., Zuber, J., McJunkin, K., Chang, K., Malone, C.D., Dickins, R.A., Xu, Q., Hengartner, M.O., Elledge, S.J., Hannon, G.J., and Lowe, S.W. (2011). Functional identification of optimized RNAi triggers using a massively parallel sensor assay. Mol. Cell *41*, 733–746.

Fujita, N., Jaye, D.L., Geigerman, C., Akyildiz, A., Mooney, M.R., Boss, J.M., and Wade, P.A. (2004). MTA3 and the Mi-2/NuRD complex regulate cell fate during B lymphocyte differentiation. Cell *119*, 75–86.

Gray, P.A., Fu, H., Luo, P., Zhao, Q., Yu, J., Ferrari, A., Tenzen, T., Yuk, D.I., Tsung, E.F., Cai, Z., et al. (2004). Mouse brain organization revealed through direct genome-scale TF expression analysis. Science *306*, 2255–2257.

Haining, W.N., and Wherry, E.J. (2010). Integrating genomic signatures for immunologic discovery. Immunity *32*, 152–161.

Hale, J.S., Youngblood, B., Latner, D.R., Mohammed, A.U., Ye, L., Akondy, R.S., Wu, T., Iyer, S.S., and Ahmed, R. (2013). Distinct memory CD4+ T cells

with commitment to T follicular helper- and T helper 1-cell lineages are generated after acute viral infection. Immunity *38*, 805–817.

Intlekofer, A.M., Takemoto, N., Wherry, E.J., Longworth, S.A., Northrup, J.T., Palanivel, V.R., Mullen, A.C., Gasink, C.R., Kaech, S.M., Miller, J.D., et al. (2005). Effector and memory CD8+ T cell fate coupled by T-bet and eomesodermin. Nat. Immunol. *6*, 1236–1244.

Ji, Y., Pos, Z., Rao, M., Klebanoff, C.A., Yu, Z., Sukumar, M., Reger, R.N., Palmer, D.C., Borman, Z.A., Muranski, P., et al. (2011). Repression of the DNA-binding inhibitor Id3 by Blimp-1 limits the formation of memory CD8+ T cells. Nat. Immunol. *12*, 1230–1237.

Johnston, R.J., Poholek, A.C., DiToro, D., Yusuf, I., Eto, D., Barnett, B., Dent, A.L., Craft, J., and Crotty, S. (2009). Bcl6 and Blimp-1 are reciprocal and antagonistic regulators of T follicular helper cell differentiation. Science *325*, 1006–1010.

Joshi, N.S., Cui, W., Chandele, A., Lee, H.K., Urso, D.R., Hagman, J., Gapin, L., and Kaech, S.M. (2007). Inflammation directs memory precursor and short-lived effector CD8(+) T cell fates via the graded expression of T-bet transcription factor. Immunity *27*, 281–295.

Kaech, S.M., and Cui, W. (2012). Transcriptional control of effector and memory CD8+ T cell differentiation. Nat. Rev. Immunol. *12*, 749–761.

Kalia, V., Sarkar, S., Subramaniam, S., Haining, W.N., Smith, K.A., and Ahmed, R. (2010). Prolonged interleukin-2Ralpha expression on virus-specific CD8+ T cells favors terminal-effector differentiation in vivo. Immunity *32*, 91–103.

Kao, C., Oestreich, K.J., Paley, M.A., Crawford, A., Angelosanto, J.M., Ali, M.A., Intlekofer, A.M., Boss, J.M., Reiner, S.L., Weinmann, A.S., and Wherry, E.J. (2011). Transcription factor T-bet represses expression of the inhibitory receptor PD-1 and sustains virus-specific CD8+ T cell responses during chronic infection. Nat. Immunol. *12*, 663–671.

Min, I.M., Waterfall, J.J., Core, L.J., Munroe, R.J., Schimenti, J., and Lis, J.T. (2011). Regulating RNA polymerase pausing and transcription elongation in embryonic stem cells. Genes Dev. *25*, 742–754.

O'Shea, J.J., and Paul, W.E. (2010). Mechanisms underlying lineage commitment and plasticity of helper CD4+ T cells. Science *327*, 1098–1102.

Obar, J.J., Khanna, K.M., and Lefrançois, L. (2008). Endogenous naive CD8+ T cell precursor frequency regulates primary and memory responses to infection. Immunity *28*, 859–869.

Oestreich, K.J., and Weinmann, A.S. (2012). Master regulators or lineage-specifying? Changing views on CD4+ T cell transcription factors. Nat. Rev. Immunol. *12*, 799–804.

Oven, I., Brdicková, N., Kohoutek, J., Vaupotic, T., Narat, M., and Peterlin, B.M. (2007). AIRE recruits P-TEFb for transcriptional elongation of target genes in medullary thymic epithelial cells. Mol. Cell. Biol. *27*, 8815–8823.

Oxenius, A., Bachmann, M.F., Zinkernagel, R.M., and Hengartner, H. (1998). Virus-specific MHC-class II-restricted TCR-transgenic mice: effects on humoral and cellular immune responses after viral infection. Eur. J. Immunol. *28*, 390–400.

Peterlin, B.M., and Price, D.H. (2006). Controlling the elongation phase of transcription with P-TEFb. Mol. Cell *23*, 297–305.

Pipkin, M.E., and Rao, A. (2009). SnapShot: effector and memory T cell differentiation. Cell *138*, e1–e2.

Pipkin, M.E., Sacks, J.A., Cruz-Guilloty, F., Lichtenheld, M.G., Bevan, M.J., and Rao, A. (2010). Interleukin-2 and inflammation induce distinct transcriptional programs that promote the differentiation of effector cytolytic T cells. Immunity *32*, 79–90.

Poholek, A.C., Hansen, K., Hernandez, S.G., Eto, D., Chandele, A., Weinstein, J.S., Dong, X., Odegard, J.M., Kaech, S.M., Dent, A.L., et al. (2010). In vivo regulation of Bcl6 and T follicular helper cell development. J. Immunol. *185*, 313–326.

Rahl, P.B., Lin, C.Y., Seila, A.C., Flynn, R.A., McCuine, S., Burge, C.B., Sharp, P.A., and Young, R.A. (2010). c-Myc regulates transcriptional pause release. Cell *141*, 432–445.

Ravasi, T., Suzuki, H., Cannistraci, C.V., Katayama, S., Bajic, V.B., Tan, K., Akalin, A., Schmeier, S., Kanamori-Katayama, M., Bertin, N., et al. (2010). An atlas of combinatorial transcriptional regulation in mouse and man. Cell *140*, 744–752.

Rutishauser, R.L., Martins, G.A., Kalachikov, S., Chandele, A., Parish, I.A., Meffre, E., Jacob, J., Calame, K., and Kaech, S.M. (2009). Transcriptional repressor Blimp-1 promotes CD8(+) T cell terminal differentiation and represses the acquisition of central memory T cell properties. Immunity *31*, 296–308.

Shin, H., Blackburn, S.D., Intlekofer, A.M., Kao, C., Angelosanto, J.M., Reiner, S.L., and Wherry, E.J. (2009). A role for the transcriptional repressor Blimp-1 in CD8(+) T cell exhaustion during chronic viral infection. Immunity *31*, 309–320.

Vahedi, G., Kanno, Y., Sartorelli, V., and O'Shea, J.J. (2013). Transcription factors and CD4 T cells seeking identity: masters, minions, setters and spikers. Immunology *139*, 294–298.

Walsh, J.C., DeKoter, R.P., Lee, H.J., Smith, E.D., Lancki, D.W., Gurish, M.F., Friend, D.S., Stevens, R.L., Anastasi, J., and Singh, H. (2002). Cooperative and antagonistic interplay between PU.1 and GATA-2 in the specification of myeloid cell fates. Immunity *17*, 665–676.

Wherry, E.J., Blattman, J.N., Murali-Krishna, K., van der Most, R., and Ahmed, R. (2003). Viral persistence alters CD8 T-cell immunodominance and tissue distribution and results in distinct stages of functional impairment. J. Virol. *77*, 4911–4927.

Xiao, N., Eto, D., Elly, C., Peng, G., Crotty, S., and Liu, Y.C. (2014). The E3 ubiquitin ligase Itch is required for the differentiation of follicular helper T cells. Nat. Immunol. *15*, 657–666.

Yang, C.Y., Best, J.A., Knell, J., Yang, E., Sheridan, A.D., Jesionek, A.K., Li, H.S., Rivera, R.R., Lind, K.C., D'Cruz, L.M., et al. (2011). The transcriptional regulators Id2 and Id3 control the formation of distinct memory CD8+ T cell subsets. Nat. Immunol. *12*, 1221–1229.

Yusuf, I., Kageyama, R., Monticelli, L., Johnston, R.J., Ditoro, D., Hansen, K., Barnett, B., and Crotty, S. (2010). Germinal center T follicular helper cell IL-4 production is dependent on signaling lymphocytic activation molecule receptor (CD150). J. Immunol. *185*, 190–202.

Zhou, P., Shaffer, D.R., Alvarez Arias, D.A., Nakazaki, Y., Pos, W., Torres, A.J., Cremasco, V., Dougan, S.K., Cowley, G.S., Elpek, K., et al. (2014). In vivo discovery of immunotherapy targets in the tumour microenvironment. Nature *506*, 52–57.

Zuber, J., Shi, J., Wang, E., Rappaport, A.R., Herrmann, H., Sison, E.A., Magoon, D., Qi, J., Blatt, K., Wunderlich, M., et al. (2011). RNAi screen identifies Brd4 as a therapeutic target in acute myeloid leukaemia. Nature *478*, 524–528.